RSC Advances

PAPER

View Article Online
View Journal | View Issue

Cite this: *RSC Adv.*, 2024, **14**, 1464

A simple 'turn-on' fluorescence chemosensor for Al(III) detection in aqueous solution and solid matrix†

Cuiping Yang and Jianbo Zhao *

Received 26th September 2023
Accepted 19th December 2023

DOI: 10.1039/d3ra06558h

rsc.li/rsc-advances

A simple fluorescence chemosensor of **FHS-OH** based on salicylaldehyde Schiff base was developed *via* a one-step reaction, which achieved a fast and highly selective response for Al(III). Mechanism studies showed that when **FHS-OH** was exposed to Al(III) with 1 : 2 binding stoichiometry in an aqueous solution at neutral pH, C=N isomerization and PET processes were limited, resulting in a 'turn-on' fluorescence response with a low detection limit of 63 nmol L^{-1} and a satisfying linear range of 0.0–20.0 μmol L^{-1}. Compared to traditional detection methods for Al(III), fluorometry using **FHS-OH** has several advantages, including simplicity, quick response, and capability of real-time detection. More importantly, the detection of Al(III) on a solid matrix (test paper) was successfully achieved. After the addition of Al(III), a significant emission colour change from green to bright blue was observed by the naked eye owing to the intrinsic aggregation-induced emission (AIE) characteristic of **FHS-OH**.

1 Introduction

Aluminium is the third most abundant element in the earth's crust and the most abundant metallic element, constituting about 8% of the total mineral composition. It is a highly toxic metal element for the human body. The accumulation of excessive aluminium can result in serious effects on the brain, liver, and reproductive system. Aluminium is usually found in the form of Al(III) in nature and living organisms. The World Health Organization (WHO) recommends an average dietary intake of Al(III) of around 3–10 mg day^{-1} and limits the concentration in drinking water to 7.41 μmol L^{-1}.[1] Owing to its noteworthy effect on human health, research investigating reliable methods for the detection of Al(III) is gaining much attention.[2,3] Fluorometry for the detection of Al(III), which offers simplicity, sensitivity, selectivity, and real-time nondestructive detection, has attracted significant attention compared to traditional instrumental analytical methods, such as atomic absorption spectrometry and potentiometric titration.[4–9]

However, most reported Al(III) fluorescent probes have been used in pure organic solvents or organic/H_2O mixed solutions.[10–17] This is because of the aggregation-caused quenching (ACQ) of most conventional fluorescent molecules. They typically exhibit strong fluorescence in the dispersed state but weak or no fluorescence in the aggregated state, which limits their applications. In addition, Al(III) is susceptible to hydrolysis, has a weak coordination ability, and is prone to interference from trivalent ions, such as Fe(III) and Cr(III), with similar electronic structures during the detection process.[8] These factors limit the detection of Al(III) in pure water under neutral conditions. Unfortunately, physiological processes typically occur in environments with high water content and neutral pH, making the detection of Al(III) in drinking water and biological samples challenging. Furthermore, the development of Al(III) chemosensors is limited by intricate synthesis procedures, low yields, and high expenses.

Aggregation-induced emission is a luminescence characteristic that is opposite to ACQ.[18–21] AIE luminogens emit little or no light when dissolved in a benign organic solvent, but emit significantly more light when aggregated or solidified (usually in a poor solvent, such as water). AIE offers a basic remedy for the ACQ effect of the traditional probes and has been highly valued in the design and fabrication of fluorescent probes in physiological samples owing to their typically high signal-to-noise ratio and reliable photostability.

Herein, we report a novel fluorescent 'turn-on' probe **FHS-OH** with salicylaldehyde moieties, which could be used to recognize Al(III) in pure water aqueous solution at pH 7.4. **FHS-OH** is rich in N and O atoms, which favours coordination with Al(III), resulting in intense fluorescence enhancement. Moreover, **FHS-OH** was successfully used to detect Al(III) in real water samples and fluorescent test papers.

2 Experimental

2.1. Reagents

All the raw materials used in this work were of analytical grade and used without further purification. 2,4-

School of Chemistry and Chemical Engineering, Tarim University, Alar 843300, P. R. China. E-mail: zjb1102@outlook.com

† Electronic supplementary information (ESI) available. See DOI: https://doi.org/10.1039/d3ra06558h

Dihydroxybenzaldehyde and 2-furoic hydrazide were purchased from Energy Chemical Co., Anhui, China. Unless otherwise noted, all the other materials were purchased from Sinopharm Chemical Reagent Beijing Co., Beijing, China. Deionized water (distilled) was used throughout the experiments. A phosphate buffer solution (PBS, 10 mmol L^{-1}) was obtained by adding an appropriate amount of HCl/NaOH, which was modulated using the pH meter to monitor the pH values.

2.2. Instruments

NMR spectra were recorded on a Bruker 600 Avance NMR spectrometer operated at 600 MHz. Fluorescence spectra were obtained on an F-7000 fluorescence spectrophotometer with a 1 cm cuvette. Absorption spectra were obtained on a UV/vis spectrophotometer with a 1 cm cuvette. Dynamic Light Scattering (DLS) experiments were performed using a NanoPlus-3 dynamic light scattering particle size/zeta potential analyser. All the pH measurements were carried out using a PHS-3C pH meter. The photographs were taken on a Nikon Z5 camera.

2.3. Analytical procedure

2.3.1 Fluorescence titration experiments. **FHS-OH** (12.5 mg, 0.05 mmol) was dissolved in DMSO (5 mL) to prepare the stock solution (10 mmol L^{-1}). 10 μL of **FHS-OH** stock solution was added to 2 mL of PBS (10 mmol L^{-1}, pH 7.4) to give a final concentration of 50 μmol L^{-1}. $Al(NO_3)_3$ (10.65 mg, 0.05 mmol) was dissolved in deionized water (5 mL) to prepare a stock solution (10 mmol L^{-1}). 2–30 μL of Al(III) stock solution were transferred to the **FHS-OH** (50 μmol L^{-1}, 2 mL) as prepared above. After mixing well, the fluorescence titration experiments were performed in a 1 cm cuvette at 25 °C. For the time-dependent fluorescence experiments, the fluorescence spectra were recorded immediately after the solutions were well mixed. Excitation was performed at 374 nm.

2.3.2 Competition with other metal ions. **FHS-OH** (12.5 mg, 0.05 mmol) was dissolved in DMSO (5 mL) to prepare the stock solution (10 mmol L^{-1}). 10 μL of **FHS-OH** stock solution was added to 2 mL of PBS (10 mmol L^{-1}, pH 7.4) to produce a final concentration of 50 μmol L^{-1}. Stock solutions of various metal ions of Al(III), Li(I), Na(I), K(I), Mg(II), Ca(II), Ba(II), Cr(III), Mn(II), Fe(III), Co(II), Ni(II), Cu(II), Ag(I), Zn(II), Cd(II), and Pb(II) (100 mmol L^{-1}) were prepared in deionized water, similar to the preparation of the Al(III) stock solution, as discussed above. Then, 40 μL of each metal stock solution (100 mmol L^{-1}) was transferred to the **FHS-OH** (50 μmol L^{-1}, 2 mL) prepared above to give a final concentration of 2 mmol L^{-1}. After well mixing, fluorescence experiments were performed in a 1 cm cuvette at 25 °C. Excitation was performed at 374 nm.

2.3.3 UV-vis experiments. **FHS-OH** (12.5 mg, 0.05 mmol) was dissolved in DMSO (5 mL) to prepare a stock solution (10 mmol L^{-1}). 10 μL of **FHS-OH** stock solution was added to 2 mL of PBS (10 mmol L^{-1}, pH 7.4) to give a final concentration of 50 μmol L^{-1}. UV-vis spectra were recorded in the range of 300–700 nm in a 1 cm cuvette at 25 °C. Subsequently, 40 μL of the Al(III) stock solution (100 mmol L^{-1}) was transferred to the **FHS-OH** (50 μmol L^{-1}, 2 mL), as prepared above, to have a final concentration of 2 mmol L^{-1}. After mixing well, UV-vis spectra were recorded in the range of 300–700 nm in a 1 cm cuvette at 25 °C.

2.3.4 Job plot experiments. **FHS-OH** (12.5 mg, 0.05 mmol) was dissolved in DMSO (5 mL) to prepare a stock solution (10 mmol L^{-1}). Subsequently, 0, 1, 2, 3, 4, 5, 6, 7, 8, 9, and 10 μL of the **FHS-OH** stock solution (10 mmol L^{-1}) were taken and transferred to 2 mL of PBS (10 mmol L^{-1}, pH 7.4). $Al(NO_3)_3$ (10.65 mg, 0.05 mmol) was dissolved in deionized water (5 mL) to form a stock solution (10 mmol L^{-1}). 10, 9, 8, 7, 6, 5, 4, 3, 2, 1, and 0 μL of Al(III) stock solution (10 mmol L^{-1}) were taken and transferred to the **FHS-OH** solution prepared above. The total concentrations of **FHS-OH** and Al(III) were 50 μmol L^{-1}. Excitation was performed at 374 nm.

2.3.5 Fluorescence experiments at different pH levels. PBS (10 mmol L^{-1}) at different pH values were obtained by adding appropriate amounts of HCl/NaOH. 10 μL of **FHS-OH** stock solution (10 mmol L^{-1}) was added to 2 mL of PBS (10 mmol L^{-1}, pH = 1.0–14.0) as described above to give a final concentration of 50 μmol L^{-1}. Fluorescence experiments were performed in a 1 cm cuvette at 25 °C. Then, 40 μL of Al(III) stock solution (100 mmol L^{-1}) was transferred to the **FHS-OH** (50 μmol L^{-1}, 2 mL) prepared above to make a final concentration of 2 mmol L^{-1}. After well mixing, fluorescence experiments were performed in a 1 cm cuvette at 25 °C. Excitation was performed at 374 nm.

2.3.6 Fluorescence experiments in varying water fractions. 0, 200, 400, 600, 800, 1000, 1200, 1400, 1600, 1800, and 2000 μL of PBS (10 mmol L^{-1}, pH 7.4) were taken and transferred to vials. Subsequently, 2000, 1800, 1600, 1400, 1200, 1000, 800, 600, 400, 200, and 0 μL of absolute ethanol were added sequentially to the vials. Each vial had a total volume of 2 mL solution with varying water fractions (f_w: 0–99%). **FHS-OH** (12.5 mg, 0.05 mmol) was dissolved in DMSO (5 mL) to prepare the stock solution (10 mmol L^{-1}). Then, 10 μL of **FHS-OH** stock solution was added to 2 mL of the mixed solutions, as prepared above, to give a final concentration of 50 μmol L^{-1}. After mixing well for 20 minutes, the fluorescence spectra were recorded.

2.4. Synthesis and characterization

The synthetic routes for **FHS-OH** are shown in Scheme 1.

2,4-Dihydroxybenzaldehyde (0.28 g, 2 mmol) and 2-furoic hydrazide (0.25 g, 2 mmol) were dissolved in 20 mL absolute ethanol. Then, the mixture was stirred and refluxed at 80 °C for 30 minutes. After cooling the mixture to room temperature, the solvent was removed under reduced pressure. After that, the crude product was recrystallized from ethanol, obtaining a light yellow solid (393 mg, yield 80%). ^{1}H NMR (DMSO-d_6) δ (ppm): 11.94 (s, 1H), 11.33 (s, 1H), 9.97 (s, 1H), 8.51 (s, 1H), 7.95 (s, 1H), 7.28 (dd, J = 14.4 Hz, 2H), 6.70 (s, 1H), 6.37 (d, J = 12.0 Hz, 1H), 6.32 (s, 1H). ^{13}C NMR (DMSO-d_6) δ (ppm): 161.22, 159.80, 154.19, 149.64, 137.66, 136.54, 135.61, 134.22, 133.09, 133.04, 131.76, 129.99, 129.22, 129.07, 128.65, 122.04, 121.87, 119.66, 113.02, 110.63. Detailed characterization data can be found in the ESI.†

2.5. Preparation of test paper

The filter paper was placed into an ethanol solution of **FHS-OH** (50 mmol L^{-1}) for 20 minutes. Then, the filter paper was dried

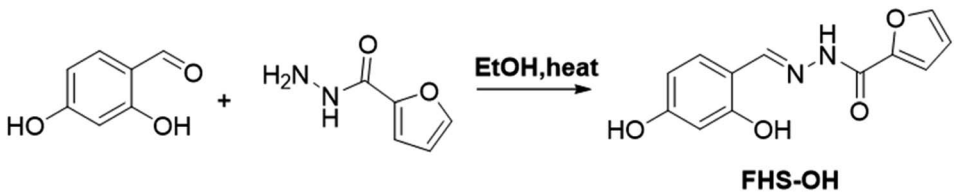

Scheme 1 Synthetic route of FHS-OH.

in air for 30 minutes at room temperature. In this way, a test paper was obtained.

3 Results and discussion

3.1. Fluorescence response of FHS-OH toward Al(III)

The fluorescence response of **FHS-OH** to Al(III) in a neutral aqueous solution buffered using 10 mmol L^{-1} of the phosphate buffer solution (PBS, pH 7.4) at 25 °C was first carried out. As seen in Fig. 1A, there was no fluorescence emission of **FHS-OH** when Al(III) was not present. Al(III) caused a brilliant blue fluorescence to arise, with the emission peak occurring at 438 nm. After the addition of Al(III), the emission rose progressively, reaching a 106-fold enhancement in about 20 minutes. The fluorescence 'turn-on' response could be clearly observed by the naked eye under UV light (Fig. 1A inset), indicating that **FHS-OH** has the potential to be used as a 'turn-on' fluorescence probe for the detection of Al(III) in the aqueous solution at pH 7.4. More importantly, when EDTA was added to the solution of **FHS-OH** and Al(III), the fluorescence emission at 438 nm quenched, again leaving a characteristic fluorescence emission of **FHS-OH** (Fig. 1B), which suggested that the combination between **FHS-OH** and Al(III) was reversible.

To verify whether **FHS-OH** can be used for the quantitative detection of Al(III), a fluorescence titration experiment was performed. When more than 2.0 equiv. Al(III) was added, the fluorescence intensity at 438 nm reached the maximum and varied very slightly, indicating that the binding ratio of **FHS-OH** to Al(III) might be 1 : 2 (Fig. 2A). Furthermore, the calibration curve for the determination of Al(III) was constructed (Fig. 2B). A satisfying linear range of 0.0–20.0 μmol L^{-1} was achieved with a correlation coefficient of $R^2 = 0.99$ ($n = 3$). The detection limit was calculated to be 63 nmol L^{-1} based on the equation of $C_{DL} = 3S_b/m$ (S_b is the standard deviation from 10 blank solutions while m represents the slope of the calibration curve), which is defined by IUPAC. The detection limit (LOD) of **FHS-OH** is in the normal range compared to some reported molecular probes for the detection of Al(III) in recent years. These results suggested that **FHS-OH** has the potential to be used in the quantitative detection of Al(III) in aqueous physiological samples. Based on the Benesi–Hildebrand equation, the binding constant K of **FHS-OH** with Al(III) was determined as 3.32×10^4 M^{-1} (Fig. S3†).

The ability to achieve a highly selective response to analytes is an important characteristic of a good chemical sensor. The selectivity of **FHS-OH** to Al(III) was further investigated. Fluorescence intensities of **FHS-OH** at 438 nm in the presence of different metal ions including Al(III), Li(I), Na(I), K(I), Mg(II), Ca(II), Ba(II), Cr(III), Mn(II), Fe(III), Co(II), Ni(II), Cu(II), Ag(I), Zn(II), Cd(II), and Pb(II) exhibited a weak fluorescence emission. As can be seen in Fig. 2C, only Al(III) caused a significant enhancement compared to other metal ions, which proves that Al(III) showed a strong binding affinity towards **FHS-OH**, indicating an excellent selectivity of **FHS-OH** to Al(III).

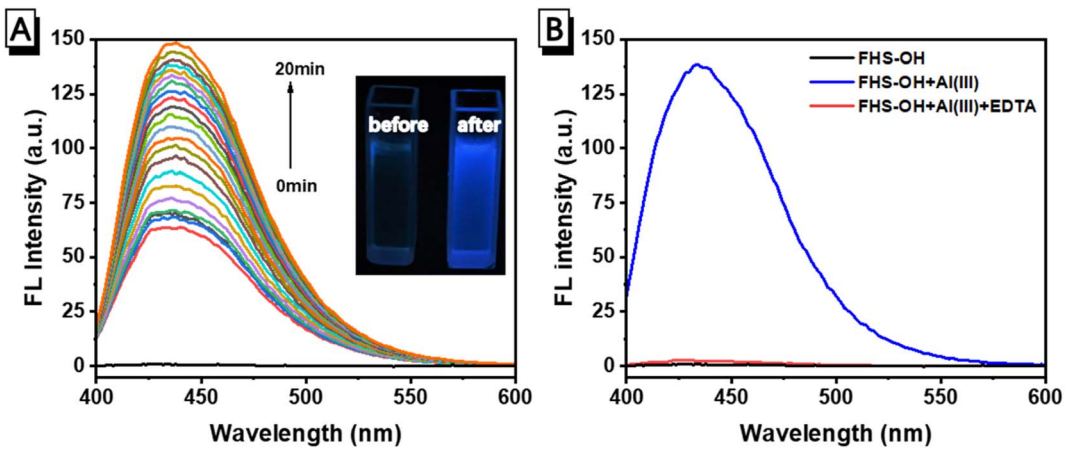

Fig. 1 (A) Fluorescence spectra and photographs of **FHS-OH** before and after the addition of Al(III) (inset). (B) Fluorescence spectra of **FHS-OH** in the absence and presence of 40 equiv. of Al(III) and 80 equiv. of EDTA. Conditions: 99% H_2O/EtOH (v/v) at pH 7.4 buffered with 10 mmol per L PBS; the concentrations of **FHS-OH** and Al(III) were 50 μmol L^{-1} and 2 mmol L^{-1}, respectively. Excitation was performed at 374 nm. The photograph was taken under an irradiation of 365 nm UV light.

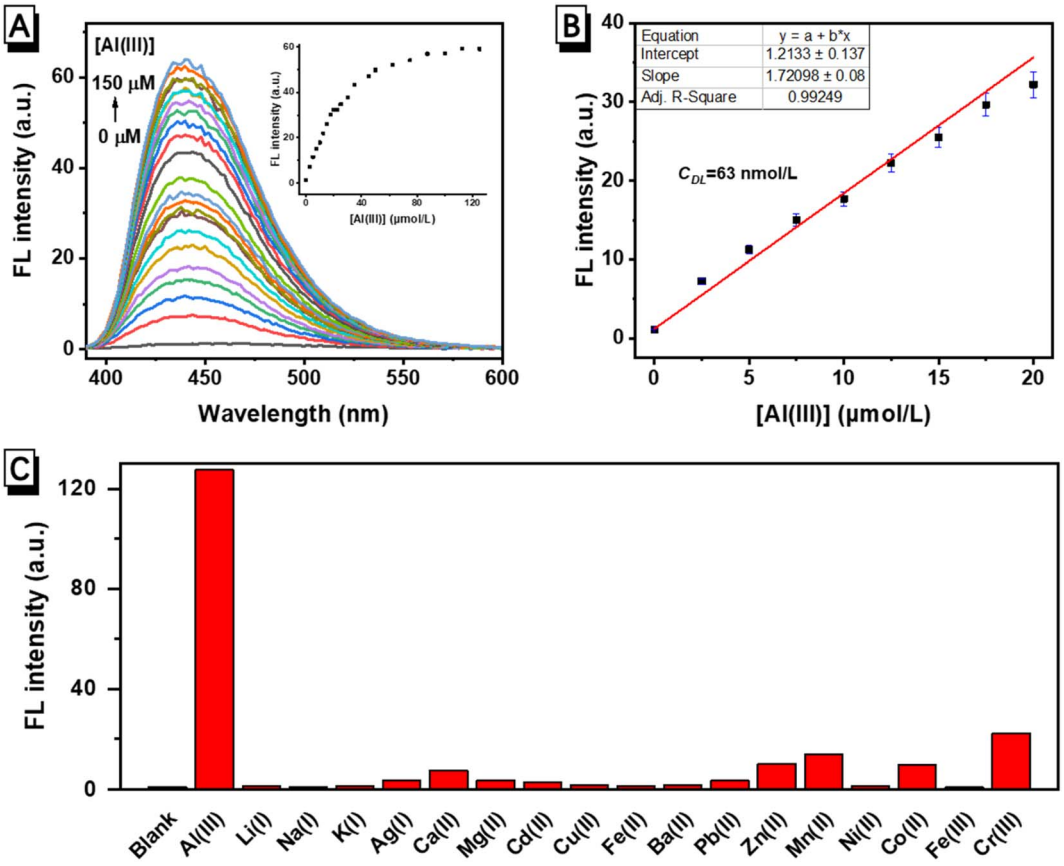

Fig. 2 (A) Fluorescence spectra of **FHS-OH** upon the addition of 0–150 μmol per L Al(III). Inset: the fluorescence intensities at 438 nm as a function of Al(III) concentration. (B) Average fluorescence intensities at 438 nm of the three measurements as a function of Al(III) concentration. (C) The fluorescence intensities at 438 nm in the presence of 2 mmol L^{-1} of different metal ions. Conditions: 99% H_2O/EtOH (v/v) at pH 7.4 buffered using 10 mmol per L PBS, the concentration of **FHS-OH** was 50 μmol L^{-1}. Excitation was performed at 374 nm.

3.2. Response mechanism of FHS-OH toward Al(III)

The superior selectivity of **FHS-OH** can be attributed to the higher charge density and smaller ionic radius of Al(III), which allows the formation of a stable coordination structure between **FHS-OH** and Al(III).[17,22] Salicylaldehyde Schiff base compounds are generally considered to be poorly fluorescent, partly due to the isomerization of the C=N double bond in the excited state and partly due to the presence of a photo-induced electron transfer (PET) process within the molecule. A possible mechanism to explain the 'turn-on' fluorescence response of **FHS-OH** towards Al(III) is proposed in Scheme 2. The lone pair electron of nitrogen from C=N can be freely transferred to the excited state fluorophore, resulting in fluorescence quenching.[23–25] When the nitrogen and oxygen atoms of **FHS-OH** coordinate with Al(III), the electron-donating ability decreases, and the PET effect is constrained, leading to a notable enhancement of fluorescence emission at 438 nm.[26–33] Besides PET and C=N isomerization

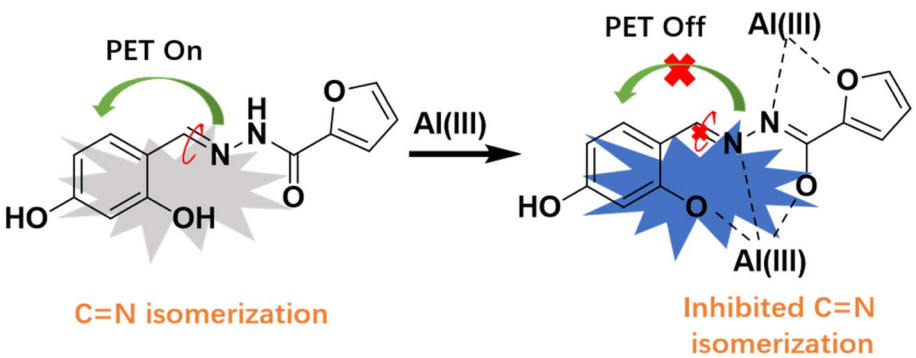

Scheme 2 Proposed mechanism of **FHS-OH** in Al(III) detection.

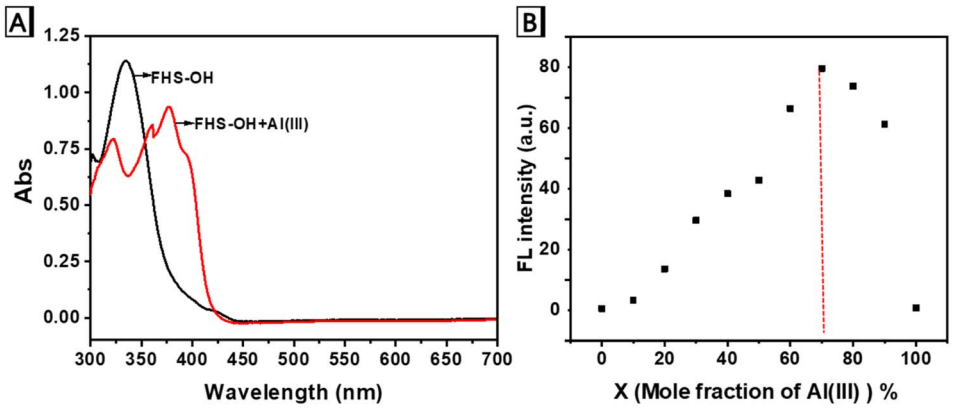

Fig. 3 (A) Absorption spectra of FHS-OH before and after the addition of Al(III). Conditions: 99% H_2O/EtOH (v/v) buffered using 10 mmol per L PBS at pH 7.4. The concentrations of FHS-OH and Al(III) were 50 μmol L^{-1} and 2 mol L^{-1}, respectively. (B) Job plot data for evaluating the stoichiometry of the FHS-OH-Al complex. Conditions: 99% H_2O/EtOH (v/v) buffered with 10 mmol per L PBS at pH 7.4. The total concentration of FHS-OH and Al(III) was 50 μmol L^{-1}. Excitation was performed at 374 nm.

could also be involved in the fluorescence enhancement. In compounds with an unbridged C=N structure, C=N isomerization is the dominant excited state decay process. As a result, the free sensor **FHS-OH** has very weak fluorescence. In contrast, compounds with a covalently bridged C=N structure are known to show fluorescence intensity due to the restriction of C=N isomerization in the excited states. Likewise, Al(III) binding can lock the C=N bond of **FHS-OH** and inhibit the C=N isomerization. The molecular structure changed from flexible to rigid, resulting in a dramatic increase in the fluorescence intensity.[34–41]

To support the hypothesis, a series of experiments were carried out. As shown in the absorption spectra (Fig. 3A), **FHS-OH** showed a significant absorption peak at 336 nm. With the addition of Al(III), the absorption at 336 nm gradually decreased, accompanied by three new absorption peaks at 323, 359, and 377 nm, respectively. An isosbestic point was observed at 353 nm, potentially indicating the formation of novel coordination between **FHS-OH** and Al(III). In addition, the Job's plot analysis was performed to evaluate the binding of **FHS-OH** and Al(III) (Fig. 3B), with the highest fluorescence intensity achieved when Al(III) accounted for 70%, consistent with a 1 : 2 metal-to-ligand ratio.

3.3. Analytical performance of FHS-OH toward Al(III) in real water samples

In order to determine the optimum pH for Al(III) detection, the fluorescence spectra of **FHS-OH** before and after the addition of Al(III) at different pH levels were examined.[42] As shown in Fig. 4, the fluorescence intensity of **FHS-OH** was very weak in pH 1.0–14.0. Interestingly, when Al(III) was added, fluorescence intensity was not affected under strongly acidic conditions (pH = 1.0–2.0). This phenomenon could be attributed to the protonation of oxygen and nitrogen atoms of **FHS-OH**, which inhibited the coordination with Al(III).[43] On the contrary, an intense fluorescence enhancement can be observed under weak acid and neutral conditions, which can be attributed to the formation of **FHS-OH** and Al(III) chelate polymers (pH = 4.0–8.0). At pH > 8.0, the fluorescence intensity of the system again showed an overall decreasing trend with increasing pH, which may be due to two possible reasons. One is the deprotonation of **FHS-OH** under alkaline conditions. The other is the formation of $Al(OH)_3$ precipitates, which can prevent the formation of chelate polymers.[44,45] These results indicate that the neutral environment is favorable for the chelation of **FHS-OH** with Al(III). In particular, the maximum signal-to-noise ratio is around pH 7.4, indicating the optimal detection conditions for Al(III), which offers the possibility of achieving bio-detection.

Based on the above experimental results, the optimal conditions were obtained as: 50 μmol per L **FHS-OH** was used as a probe in a 10 mmol per L PBS at pH 7.4. The fluorescence intensity was measured at the excitation/emission wavelengths of 374 nm/438 nm after the reaction with Al(III) for 20 minutes at room temperature. Under optimized conditions, **FHS-OH** was applied to detect Al(III) in real drinking water and tap water

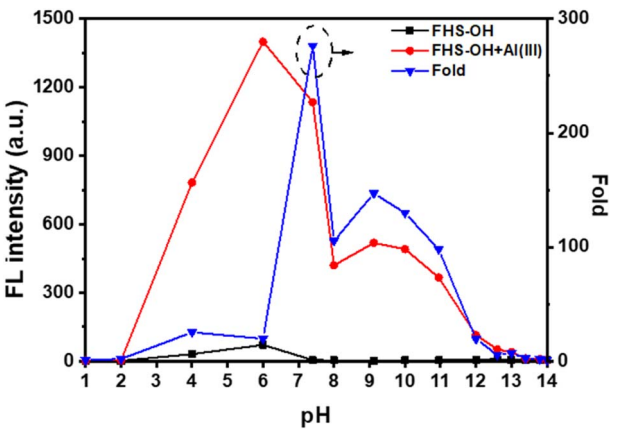

Fig. 4 Fluorescence intensities at 438 nm of FHS-OH in the absence and presence of Al(III) at different pH. Conditions: the concentrations of FHS-OH and Al(III) were 50 μmol L^{-1} and 2 mol L^{-1}, respectively. Excitation was performed at 374 nm.

Table 1 Detection of Al(III) in real water samples

Sample	Al(III) added (μmol L^{-1})	Al(III) found (μmol L^{-1})	Recovery (%)	R.S.D. ($n = 3$) (%)
Drinking water	0.00	0.56	—	1.21
	10.00	10.63	100.7	0.98
Tap water	0.00	6.73	—	0.79
	10.00	17.01	102.8	1.11
Laker water	0.00	9.96	—	0.87
	10.00	19.85	98.9	1.02

samples by the proposed method, which showed satisfactory recovery and R.S.D. values for all the water samples, demonstrating the potential applications of **FHS-OH** in real sample analysis (Table 1).

Owing to the advantages of rapid detection and good selectivity, test papers based on **FHS-OH** for Al(III) detection were successfully fabricated. Interestingly, **FHS-OH** on the filter paper exhibited green fluorescence rather than no emission under UV-light irradiation. When exposed to Al(III) with certain concentrations, the fluorescence emission changed from green to blue. When the Al(III) concentration was higher than 5 mmol L^{-1}, strong blue fluorescence could be directly observed by the naked eye upon UV-light irradiation (Fig. 5A). More importantly, as illustrated in Fig. 5B, strong blue fluorescence was only observed with the addition of Al(III), indicating that the test papers exhibited good selectivity for Al(III) over other tested metal ions.

3.4. AIE properties of FHS-OH

It has been reported that luminogens based on salicylaldehyde Schiff bases usually exhibit AIE properties.[46–49] In order to understand whether the green fluorescence of **FHS-OH** on test papers is derived from its AIE property, the fluorescence intensity of **FHS-OH** in H_2O/EtOH (water fraction f_w: 0–99%, v/v) was firstly investigated. Normally, H_2O is a poor solvent, whereas EtOH is a good solvent for organic compounds. As can be seen in Fig. 6A and B, there was no fluorescence emission of **FHS-OH** in pure EtOH, whereas a green fluorescence with an emission peak at about 478 nm increased sharply up to f_w = 50% with maximum fluorescence intensity and a 151-fold enhancement compared to that of the EtOH solution. Upon further addition of H_2O to the mixture, the fluorescence emission slowly decreased, indicating its AIE property. In addition, dynamic light scattering (DLS) data were collected, which revealed the presence of nanoscale particles in the **FHS-OH** solution (Fig. S4†). The above results showed that the intense

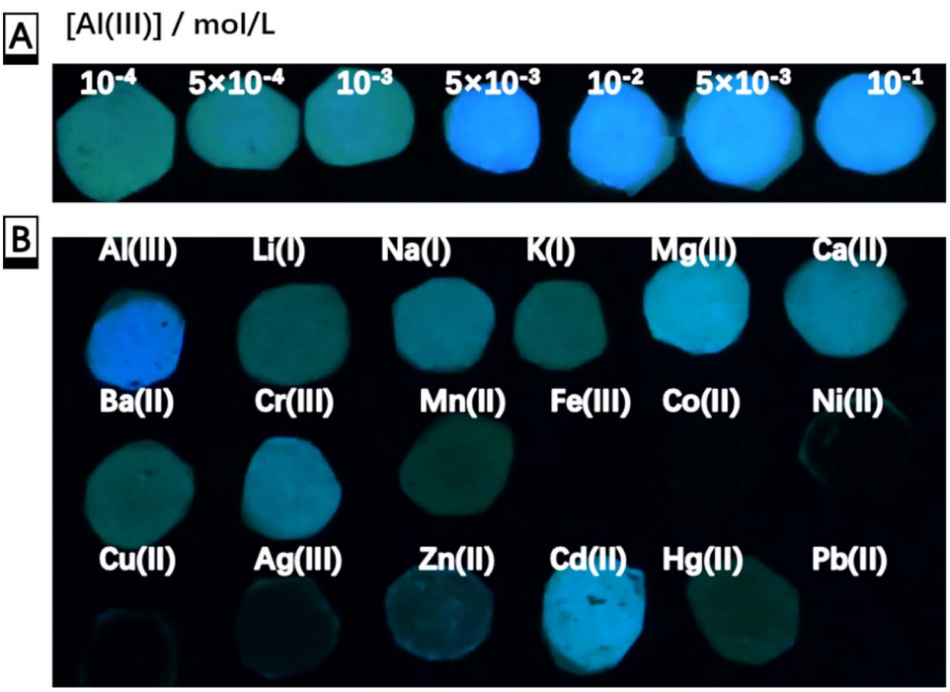

Fig. 5 (A) Photographs of the test papers based on FHS-OH for the detection of Al(III) at different concentrations under irradiation with a 365 nm UV lamp. (B) Photographs of test papers based on FHS-OH for the detection of different metal ions in aqueous solutions (5 mmol L^{-1}) under irradiation with a 365 nm UV lamp.

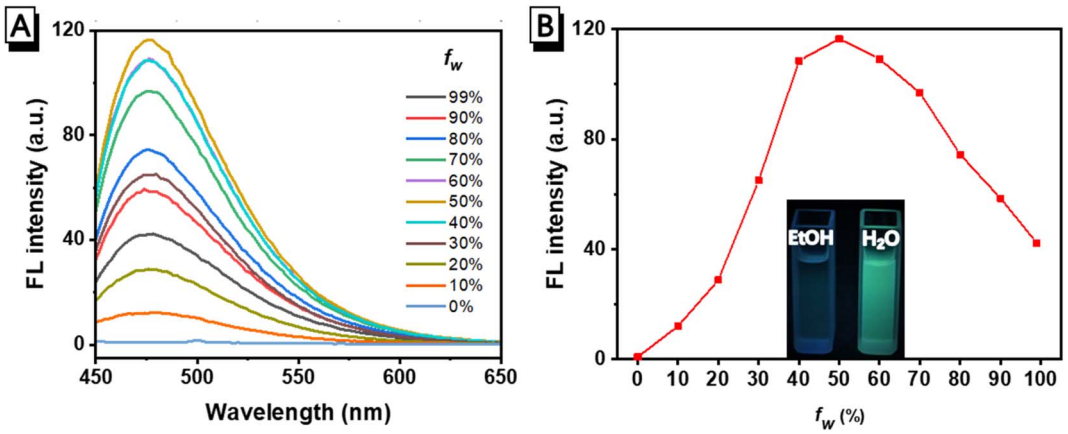

Fig. 6 (A) Fluorescence spectra of **FHS-OH** in H_2O/EtOH mixtures with different water fractions. (B) Fluorescence intensity of **FHS-OH** at 478 nm as a function of f_w. Inset: photographs of **FHS-OH** in EtOH and 50% H_2O/EtOH (v/v). Conditions: 10 mmol per L PBS at pH 7.4; the concentration of **FHS-OH** was 50 μmol L^{-1}. Excitation was performed at 374 nm. The photograph was taken under an irradiation of 365 nm UV light.

Table 2 Comparison of other reported fluorescence probes based on a Schiff base for Al(III) detection

Probes	LOD (nmol L^{-1})	Testing media	pH range	Reference
1	5.2	HMTA	5.8	10
2	31	DMF : H_2O (1 : 9)	3.0–8.0	11
3	1850	H_2O : DMF (1 : 4)	7.0	12
4	6.7	CH_3CN : H_2O (1 : 1)	6.8–7.4	13
5	42.6	PBS : DMSO (3 : 1)	5.0–8.0	14
6	3	DMSO : HEPES (9 : 1)	5.0–8.0	15
7	256	MeOH	—	16
8	1.11	EtOH	—	17
This work	63	PBS	7.4	—

fluorescence of **FHS-OH** in the solid matrix was attributed to aggregation, *i.e.*, AIE fluorescence.

3.5. Comparison with other reported Al(III) chemosensors

To further evaluate the detection performance of **FHS-OH**, a brief comparison of the sensing performance of **FHS-OH** with other reported fluorescence probes based on Schiff base for Al(III) recognition is listed in Table 2. As shown in Table 2, despite numerous investigations on sensing Al(III) in organic solvents or organic/H_2O, probes that function in aqueous solutions are still limited. In this work, the **FHS-OH** can be used to detect Al(III) in a pure aqueous medium. In addition, in comparison with other reported probes, **FHS-OH** possessed other outstanding superiorities in terms of the detection limit, and pH application range, indicating that **FHS-OH** can act as a promising fluorescence probe for Al(III) detection.

4 Conclusions

In summary, a 'turn-on' fluorescent probe **FHS-OH** for Al(III) detection based on salicylaldehyde Schiff base was facilely prepared *via* a one-step condensation reaction with inexpensive raw materials. **FHS-OH** exhibited a highly sensitive and selective fluorescence response towards Al(III) with a LOD of 63 nmol L^{-1}. Fluorescence experiments and Job's plot data showed that **FHS-OH** and Al(III) formed a 1 : 2 complex with an obvious color change from colorless to blue in an aqueous solution. More importantly, **FHS-OH** was successfully used to establish an effective method for the rapid detection of Al(III) on test paper with an obvious color change from green to blue by the naked eye due to the intrinsic AIE characteristic of **FHS-OH**. This work provides a new strategy for the trace analysis of Al(III) in a pure water system at neutral conditions.

Conflicts of interest

There are no conflicts to declare.

Acknowledgements

This work was supported by the National Natural Science Foundation of China (Grant No. 22268038 and 21865026), the Presidential Research Fund of Tarim University (No. TDZKSS202129).

References

1 WHO, *Guidelines for Drinking-Water Quality: Fourth Edition Incorporating the First and Second Addenda (who.int)*, 2022.
2 G. Khairy, A. Amin, S. Moalla, A. Medhat and N. Hassan, *Anal. Sci.*, 2023, **39**, 1307–1316.
3 Y. Liu, A. Bi, T. Gao, X. Cao, F. Gao, P. Rong, W. Wang and W. Zeng, *Talanta*, 2019, **194**, 38–45.
4 R. Shanmugapriya, P. Kumar, C. Nandhini, K. Satheeshkumar, K. Vennila and K. Elango, *Methods Appl. Fluoresc.*, 2022, **10**, 034005–034018.
5 H. Silva, A. Mageste, S. Silva, G. Dias Ferreira and G. Ferreira, *Carbohydr. Polym.*, 2020, **230**, 115679–115686.
6 E. Oliveira, H. Santos, J. Capelo and C. Lodeiro, *Inorg. Chim. Acta*, 2012, **381**, 203–211.

7 V. Jisha, K. Arun, M. Hariharan and D. Ramaiah, *J. Phys. Chem. B*, 2010, **114**, 5912–5919.
8 Q. Wang, X. Wen and Z. Fan, *J. Photochem. Photobiol., A*, 2018, **358**, 92–99.
9 N. Chereddy, P. Nagaraju, M. Niladri Raju, V. Krishnaswamy, P. Korrapati, P. Bangal and V. Rao, *Biosens. Bioelectron.*, 2015, **68**, 749–756.
10 H. Wang, B. Wang, Z. Shi, X. Tang, W. Dou, Q. Han, Y. Zhang and W. Liu, *Biosens. Bioelectron.*, 2015, **65**, 91–96.
11 H. Peng, Y. Liu, J. Huang, S. Huang, X. Cai, S. Xu, A. Huang, Q. Zeng and M. Xu, *J. Mol. Struct.*, 2021, **1229**, 129866–129871.
12 Q. Wang, X. Wen and Z. Fan, *J. Photochem. Photobiol., A*, 2018, **358**, 92–99.
13 Y. Jiang, L. Sun, G. Ren, X. Niu, W. Hu and Z. Hu, *ChemistryOpen*, 2015, **4**, 378–382.
14 Y. Zhu, X. Gong, Z. Li, X. Zhao, Z. Liu, D. Cao and R. Guan, *Spectrochim. Acta, Part A*, 2019, **219**, 202–205.
15 I. Song, P. Torawane, J. Lee, S. Warkad, A. Borase, S. Sahoo, S. Nimse and A. Kuwar, *Mater. Adv.*, 2021, **2**, 6306–6314.
16 N. Kshirsagar, R. Sonawane, P. Patil, J. Nandre, P. Sultan, S. Sehlangia, C. Pradeep, Y. Wang, L. Chen and S. Sahoo, *Inorg. Chim. Acta*, 2020, **511**, 119805–119811.
17 Y. Huang, F. Wang, S. Mu, X. Sun, Q. Li, C. Xie and H. Liu, *Spectrochim. Acta, Part A*, 2020, **243**, 118754–118761.
18 K. Li, Q. Feng, G. Niu, W. Zhang, Y. Li, M. Kang, K. Xu, J. He, H. Hou and B. Tang, *ACS Sens.*, 2018, **3**, 920–928.
19 Y. He, Y. Li, H. Su, Y. Si, Y. Liu, Q. Peng, J. He, H. Hou and K. Li, *Mater. Chem. Front.*, 2019, **3**, 50–56.
20 Y. Li, Q. Peng, S. Li, Y. Cai, B. Zhang, K. Sun, J. Ma, C. Yang, H. Hou, H. Su and K. Li, *Sens. Actuators, B*, 2019, **301**, 127139–127149.
21 C. Yang, Y. Li, J. Wang, J. He, H. Hou and K. Li, *Sens. Actuators, B*, 2019, **285**, 617–624.
22 Y. Huang, F. Wang, S. Mu, X. Sun, Q. Li, C. Xie and H. Liu, *Spectrochim. Acta, Part A*, 2020, **243**, 118754–118761.
23 G. Park, M. Lee, G. You, Y. Choi and C. Kim, *Tetrahedron Lett.*, 2014, **55**, 2517–2522.
24 J. Wang, Y. Li, K. Li, X. Meng and H. Hou, *Chem. – Eur. J.*, 2017, **23**, 5081–5089.
25 D. Xiu, J. Shi, M. Deng, H. Song, Z. Hao, Q. Feng and H. Yu, *J. Mol. Struct.*, 2021, **1243**, 130761–130767.
26 Z. Liu, W. He and Z. Guo, *Chem. Soc. Rev.*, 2013, **42**, 1568–1600.
27 H. Wang, B. Wang, Z. Shi, X. Tang, W. Dou, Q. Han, Y. Zhang and W. Liu, *Biosens. Bioelectron.*, 2015, **65**, 91–96.
28 N. Kshirsagar, R. Sonawane, P. Patil, J. Nandre, P. Sultan, S. Sehlangia, C. Pradeep, Y. Wang, L. Chen and S. Sahoo, *Inorg. Chim. Acta*, 2020, **511**, 119805–119811.
29 Y. Wu, W. Lan, S. He, X. Guo, C. Hai, X. Zhao, H. Chen, W. Long, Y. She and H. Fu, *Spectrochim. Acta, Part A*, 2023, **298**, 122760–122769.
30 T. Zhou, J. Wang, J. Xu, C. Zheng, Y. Niu, C. Wang, F. Xu, L. Yuan, X. Zhao, L. Liang and P. Xu, *Anal. Chem.*, 2020, **92**, 5064–5072.
31 C. Li, W. Hu, J. Wang, X. Song, X. Xiong and Z. Liu, *Analyst*, 2020, **145**, 6125–6129.
32 J. Zhu, L. Hu, X. Meng, F. Li, W. Wang, G. Shi and Z. Wang, *Molecules*, 2023, **28**, 3650–3662.
33 F. Bu, B. Zhao, W. Kan, L. Ding, T. Liu, L. Wang, B. Song, W. Wang and Q. Deng, *J. Photochem. Photobiol., A*, 2020, **387**, 112165–112173.
34 D. Ray and P. Bharadwaj, *Inorg. Chem.*, 2008, **47**, 2252–2254.
35 H. Jung, K. Ko, J. Lee, S. Kim, S. Bhuniya, J. Lee, Y. Kim, S. Kim and J. Kim, *Inorg. Chem.*, 2010, **49**, 8552–8557.
36 Z. Li, M. Yu, L. Zhang, M. Yu, J. Liu, L. Wei and H. Zhang, *Chem. Commun.*, 2010, **46**, 7169–7171.
37 J. Wu, W. Liu, J. Ge, H. Zhang and P. Wang, *Chem. Soc. Rev.*, 2011, **40**, 3483–3495.
38 N. Zhao, Y. Wu, R. Wang, L. Shi and Z. Chen, *Analyst*, 2011, **136**, 2277–2282.
39 J. Wu, W. Liu, X. Zhuang, F. Wang, P. Wang, S. Tao, X. Zhang, S. Wu and S. Lee, *Org. Lett.*, 2007, **9**, 33–36.
40 S. Banjan, B. Mondal, G. Vijaykumar and A. Thakur, *Inorg. Chem.*, 2017, **56**, 11577–11590.
41 A. Gupta and N. Kumar, *RSC Adv.*, 2016, **6**, 106413–106434.
42 Q. Yan, Y. Wang, Z. Wang, G. Zhang, D. Shi and H. Xu, *Spectrochim. Acta, Part A*, 2022, **279**, 121384–121392.
43 Y. Li, K. Xu, Y. Si, C. Yang, Q. Peng, J. He, Q. Hu and K. Li, *Dyes Pigm.*, 2019, **171**, 107682–107686.
44 J. Wang, Y. Li, K. Li, X. Meng and H. Hou, *Chem. – Eur. J.*, 2017, **23**, 5081–5089.
45 J. Wang, L. Feng, J. Chao, Y. Wang and S. Shuang, *Anal. Methods*, 2019, **11**, 5598–5606.
46 J. Kwon and S. Park, *Adv. Mater.*, 2011, **23**, 3615–3642.
47 W. Ding, W. Cao, X. Zheng, D. Fang, W. Wong and L. Jin, *Inorg. Chem.*, 2013, **52**, 7320–7322.
48 K. Keshav, M. Kumawat, R. Srivastava and M. Ravikanth, *Mater. Chem. Front.*, 2017, **1**, 1207–1216.
49 L. Peng, S. Xu, X. Zheng, X. Cheng, R. Zhang, J. Liu, B. Liu and A. Tong, *Anal. Chem.*, 2017, **89**, 3162–3168.